Chem. Ber. **116**, 3338 – 3346 (1983)

Hydrated Oxocarbons, III[1)]

Structural Investigations on Solid State Polymerization and Depolymerization of Thermochromic 2,6-Diorgano-1,3,5,7-tetraoxa-2,6-dibora-4,8-octalindiones

*Mohamed Yalpani**[a], *Roland Boese*[b], and *Dieter Bläser*[b]

Max-Planck-Institut für Kohlenforschung[a],
Kaiser-Wilhelm-Platz 1, D-4330 Mülheim an der Ruhr, and

Institut für Anorganische Chemie, Universität Essen-GHS[b],
D-4300 Essen 1

Received February 3, 1983

The structure of the thermochromic compound 2,6-diethyl-1,3,5,7-tetraoxa-2,6-dibora-4,8-octalindione (**1**) in the high-temperature ("hot") form **1a** and the low-temperature ("cold") form **1b** as well as that of the non-thermochromic phenyl derivative **2** have been determined by X-ray analysis. The colour change is the result of a chelation-dechelation reaction involving the boron atoms of one and the carbonyl oxygens of the neighbouring molecules. In the "cold" form the crystals consist of stacked polymer layers. The mechanism of this process is discussed.

Hydratisierte Oxokohlenwasserstoffe, III[1)]

Strukturuntersuchungen von Polymerisation und Depolymerisation im festen Zustand von thermochromen 2,6-Diorgano-1,3,5,7-tetraoxa-2,6-dibora-4,8-octalindionen

Die Struktur der thermochromen Verbindung 2,6-Diethyl-1,3,5,7-tetraoxa-2,6-dibora-4,8-octalindion (**1**) im „heißen" (**1a**) und „kalten" (**1b**) Zustand wie auch die des nichtthermochromen Phenylderivats **2** wurden röntgenographisch ermittelt. Der Farbwechsel wird durch Chelatisierung/Dechelatisierung zwischen den Bor-Atomen des einen Moleküls und den Sauerstoff-Atomen der Carbonylgruppen von Nachbarmolekülen hervorgerufen. Dies führt im „kalten" Zustand zu Kristallen aus gestapelten Polymerschichten. Der Mechanismus der Kalt/Warm-Umwandlung wird diskutiert.

In the preceding paper[1)] we described the preparation of the thermochromic (acyloxy)(alkyloxy)boranes **1** from dihydroxybutenedioic acid or from octahydroxycyclobutane. The change in colour (white/yellow) on cooling solid **1** indicates strong *intermolecular* interactions associated with chelate formation. This effect was only observed with the *n*- and *sec*-alkyl derivatives of **1**. The aryl and the *tert*-butyl derivatives, in contrast, remained colourless even when cooled to 4K. We set out to study this phenomenon

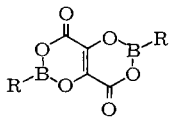

1: R = Et
2: R = Ph

0009 – 2940/83/1010 – 3338 $ 02.50/0

and to resolve this observed difference in the thermochromic behaviour by obtaining the solid state structures of both the "hot" (**1a**) and the "cold" (**1b**) form of the diethyl derivative and the room temperature structure of the phenyl derivative **2**.

The X-ray structural determination was beset by twinning problems found for the thin slates produced by high-vacuum sublimation as well as by lattice disorder of **1** at room temperature. Only when **1** was heated above 40°C or cooled below −30°C sufficient resolution of the diffraction pattern could be obtained.

Figs. 1 – 3 show the molecules of **1a**, **1b**, and **2**, respectively. Table 1 gives the intramolecular bond lengths and angles of the three structures. The two condensed rings of **1a**, **b** and **2** (cf Figs. 1 – 3) lie in a plane because of the inversion centre (0,0,0) and (0,1/2,1/2) at the middle of the double bond between C5 and C5′. **1a** (Fig. 1) and **2** at room temperature (Fig. 3) have their substituents in the same plane with a maximum deviation out of the "best" plane of 0.02 Å for C7 and C7′, and of 0.03 Å for C10 and C10′, respectively. Thus, the boron atoms of **1a** and **2** are sp^2 coordinated, which can also be derived from the bond angles in Table 1.

Table 1. Bond lengths (Å) and angles (°) of **1a**, **1b**, and **2** (standard deviations in parentheses)

1a		1b		2	
C 1 – O 2	1.365(10)	C 1 – O 2	1.273(5)	C 1 – O 2	1.389(7)
C 1 – O 6	1.200(10)	C 1 – O 6	1.271(5)	C 1 – O 6	1.187(8)
C 1 – C 5′	1.449(11)	C 1 – C 5′	1.454(5)	C 1 – C 5′	1.431(9)
O 2 – B 3	1.401(11)	O 2 – B 3	1.531(5)	O 2 – B 3	1.380(9)
B 3 – O 4	1.396(10)	B 3 – O 4	1.460(5)	B 3 – O 4	1.368(9)
B 3 – C 7	1.535(14)	B 3 – C 7	1.561(7)	B 3 – C 10	1.552(9)
		B 3 – O 6″	1.564(5)		
O 4 – C 5	1.396(10)	O 4 – C 5	1.351(5)	O 4 – C 5	1.405(7)
C 5 – C 5′	1.364(15)	C 5 – C 5′	1.339(7)	C 5 – C 5′	1.331(11)
C 7 – C 8	1.446(16)	C 7 – C 8	1.505(8)	C – C (phenyl)	1.395
O 2 – C 1 – C 5′	114.2(7)	O 2 – C 1 – C 5′	118.5(3)	O 2 – C 1 – C 5′	110.4(6)
O 2 – C 1 – O 6	119.6(7)	O 2 – C 1 – O 6	121.9(3)	O 2 – C 1 – O 6	121.4(6)
O 6 – C 1 – C 5′	126.2(8)	O 6 – C 1 – C 5′	119.6(4)	O 6 – C 1 – C 5′	128.3(6)
C 1 – O 2 – B 3	124.3(6)	C 1 – O 2 – B 3	125.9(3)	C 1 – O 2 – B 3	125.3(5)
O 2 – B 3 – O 4	119.0(7)	O 2 – B 3 – O 4	110.4(3)	O 2 – B 3 – O 4	120.7(6)
O 2 – B 3 – C 7	120.8(7)	O 2 – B 3 – C 7	111.4(4)	O 2 – B 3 – C 10	120.3(6)
		O 2 – B 3 – O 6″	104.3(3)		
O 4 – B 3 – C 7	120.1(.8)	O 4 – B 3 – C 7	115.0(3)	O 4 – B 3 – C 10	119.0(6)
		O 4 – B 3 – O 6″	107.2(3)		
		C 7 – B 3 – O 6″	107.8(4)		
C 5 – O 4 – B 3	118.8(6)	C 5 – O 4 – B 3	121.3(3)	C 5 – O 4 – B 3	117.4(5)
C 1 – C 5 – O 4	116.3(7)	C 1′– C 5 – O 4	116.6(3)	C 1′– C 5 – O 4	113.7(5)
C 5′– C 5 – O 4	121.6(9)	C 5′– C 5 – O 4	124.4(5)	C 5′– C 5 – C 1′	126.7(7)
C 5′– C 5 – C 1′	122.1(9)	C 5′– C 5 – C 1′	119.0(5)		
		C 1 – O 6 – B 3″	123.8(3)	C – C – C (phenyl)	120
B 3 – C 7 – C 8	118.2(9)	B 3 – C 7 – C 8	114.3(4)		

O 6″ is the carbonyl oxygen of the neighbouring molecule; B 3″ is the boron atom of the neighbouring molecule.

The coplanarity of the phenyl substituents with the heterooctalin ring would suggest some interactions between the π electrons of the phenyl rings and the boron atoms. However, the B – C bond distance of 1.55(1) Å is of the order of the B – C single bond (cf B3 – C7 distance in **1a** and **b**)[2]. Likewise all other interatomic distances in **1a** and **2** show no significant differences.

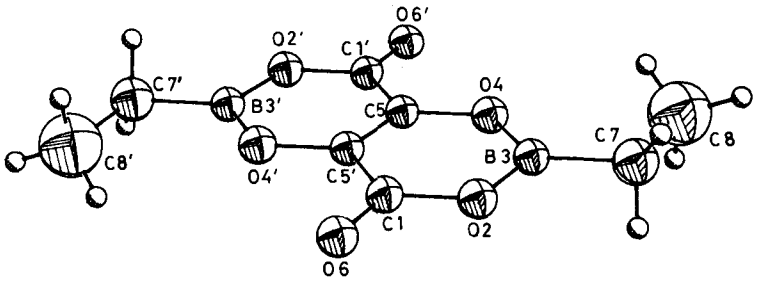

Fig. 1. Molecular structure of **1a** ("hot" form of **1**) determined at 40 °C

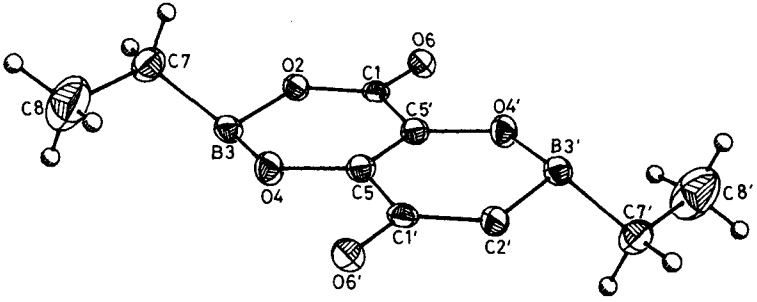

Fig. 2. Molecular structure of **1b** ("cold" form of **1**) determined at −30 °C

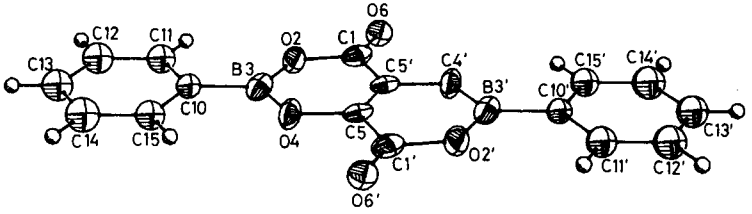

Fig. 3. Molecular structure of **2** determined at room temperature

On cooling colourless **1a** to −30 °C yellow **1b** is formed. The major change resulting within the molecule is the bending of the ethyl group (cf Fig. 2), such that the atoms C7 and C7′ are now 1.03 Å below and above the plane of the rings, and the C7 – B3 bond now forms an angle of 132.6° to the plane, being near to 180° in **1a** and **2**. Simultaneously the carbonyl oxygen O 6″ of the neighbouring molecule attaches to B3 resulting in a single bond of 1.56 Å. The sp^3 hybridisation of the boron atoms is also reflected in the bond angles formed with their neighbouring atoms (Table 1). The empty p_z orbitals of the boron atoms are apparently occupied by the lone pair electrons of the carbonyl oxygen of the neighbouring molecule.

In addition, some interatomic bond lengths are also altered: B3 – O2 and B3 – O4 have lengthened and are best regarded as single bonds while the C1 – O2 bond has shortened by 0.09 Å and thus has increased its π character. The carbonyl bond C1 – O6,

although significantly lengthened from 1.200 to 1.271 Å still retains some of it's π character.

Fig. 4

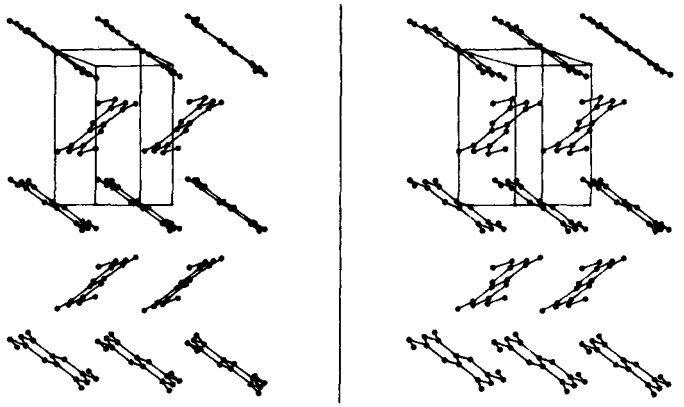

Fig. 5

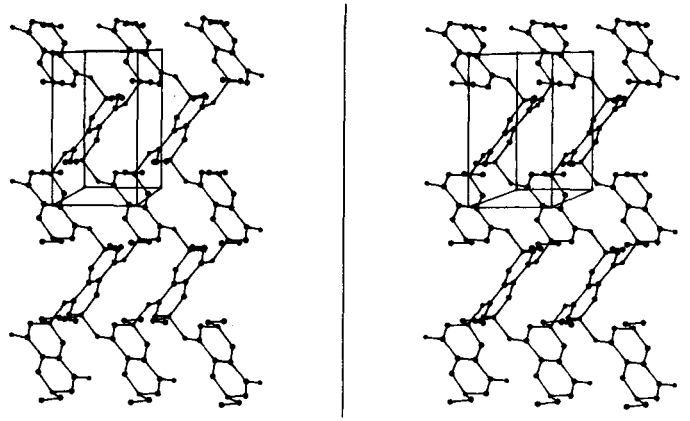

Fig. 6

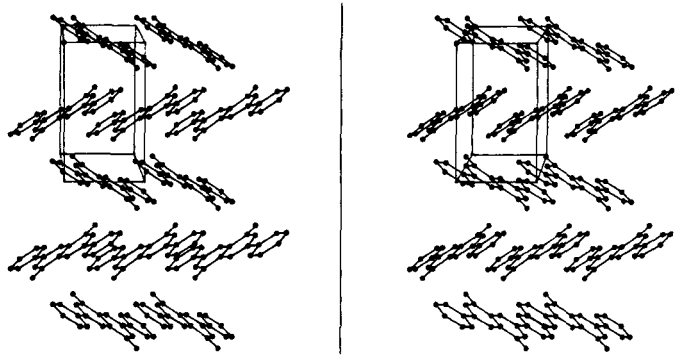

Figs. 4–6. Stereoscopic view of molecules of **1a**, **1b**, and **2** in the crystal (seen along the *a*-axis)

Figs. 4–6 show stereo plots viewed down along the *a*-axis. Fig. 4 and 6 reveal that the flat molecules are stacked in rows parallel to each other and standing nearly perpendicular to another row of molecules generated by the screw axis. The distance between the planes is 3.09 Å for **1a** and 2.98 Å for **2** while the angle between the planes of the molecules standing nearly perpendicular to each other is 73.0° for **1a** and 67.7° for **2**.

The closest intermolecular contact is that of the carbonyl oxygens of one to the boron atoms of two neighbouring molecules. In the parallel layer this distance is 3.13 Å in **1a** and 3.04 Å in **2** and in the molecules nearly perpendicular to each other the distance is 2.84 Å in **1a** and 3.23 Å in **2**. The same applies to the other carbonyl oxygen atoms of the molecule as well as to that of all neighbouring molecules throughout the crystal. Fig. 7a and b show these arrangements and the corresponding intermolecular distances and angles.

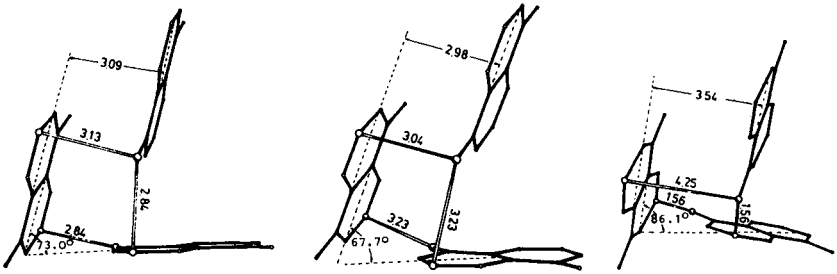

7a 7b 7c

Fig. 7a–c. Contact distances and interplanar angles for molecules of **1a**, **2**, and **1b** in the crystal

In contrast to **1a** and **2**, the "cold" form **1b** has intermolecular contact as a result of chelate formation (Fig. 5). The distance between the parallel planes has increased to 3.54 Å, the molecules have slipped and as a result the carbonyl oxygens have moved away from the boron atoms of the next parallel molecules to a distance of 4.25 Å. This is accompanied by a movement towards the boron atoms of the perpendicular molecules to a bonding distance of 1.564 Å. Finally the angle between the planes of the two perpendicular rows has increased from 73.0 to 86.1°. These changes from the "hot" **1a** to the "cold" **1b** are shown in Fig. 7c.

Thus layers of polymers are formed with their substituent ethyl groups pointing out on either side of the layers. As a result these are interlocked with the substituents of the neighbouring polymer layer. Fig. 8–10 show the molecules of **1a**, **1b**, and **2** along the *b*-axis of the lattice. Fig. 9 clearly shows how the substituents are arranged towards each other like prongs. In this Figure only one row out of the polymer layer is shown with the two neighbouring rows. In the "hot" form (Fig. 8) these prongs have been turn away from each other and shifted to the sides.

The bending and shearing movements described above are also reflected in the cell dimensions at various temperatures (Tab. 2). As the temperature is raised from −73 to −30°C, prior to the dechelation and depolymerization, the *a*-axis (along the direction of the substituents) is elongated. The arrays are pulled apart and subsequently, after passage through the thermochromic transition temperature above −30°C, sheared to

Fig. 8

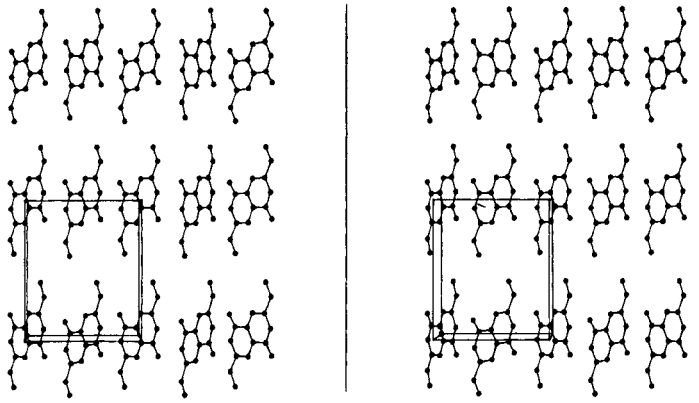

Fig. 9

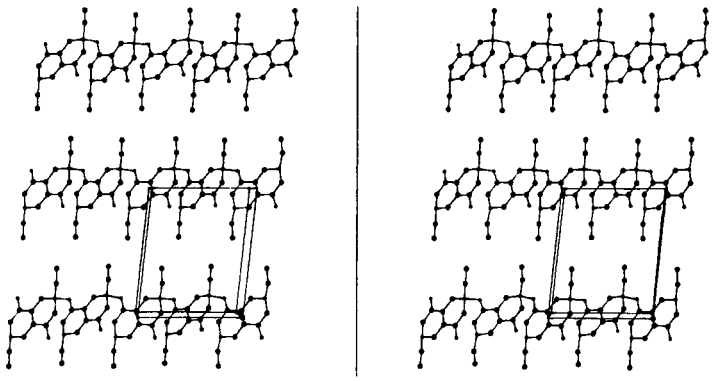

Fig. 10

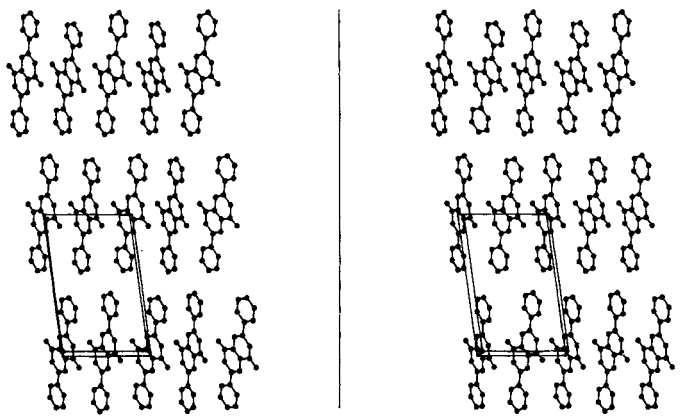

Figs. 8 – 10. Stereoscopic view of molecules of **1a**, **1b**, and **2** in the crystal (seen along the *b*-axis)

the side. This shearing process is reflected in the change of the monoclinic angle β from 98.71 to 90° when the temperature is raised from −73 to +40°C. It is reasonable to assume that with the smaller substituents methyl and ethyl the intertwining of the substituents and thus the energy required for the transition process is less than that for the higher alkyl groups. The latter substituents (see preceding paper) require considerably higher temperatures for conversion into "hot" form.

Table 2. Cell dimensions of **1a**, **1b**, and **2** at various temperatures (Standard deviations in parentheses)

Compound		**1a**		**1b**		**2**
Temperature		40°C	20°C	−30°C	−73°C	20°C
Cell dimensions	a(Å)	11.070(11)	11.007(5)	11.254(11)	10.12(3)	14.846(6)
	b(Å)	5.206(4)	5.165(1)	5.173(1)	5.407(4)	5.362(8)
	c(Å)	9.241(6)	9.210(2)	9.123(4)	9.145(7)	9.214(2)
	β(°)	90.00(3)	90.00(3)	96.01(6)	98.71(1)	97.73(3)
	V(Å^3)	532.5(7)	523.6(3)	528.2(6)	495(1)	726.8(3)

While steric factors can obviously prevent the neccessary close approach of the molecules of the *tert*-butyl derivative of **1** to lead to chelate bond formation, they cannot be the causes of the non-thermochromic behaviour in the aryl derivatives as deduced from the arrangement of the molecules of **2** (cf Figs. 6 and 10). The special requirements for a phenyl and a cyclohexyl or benzyl group should be approximately the same. The latter were found to be thermochromic with a relatively high thermochromic temperature T_{th}[1]. The assumption of a decrease of the electrophilicity of the boron atoms in the aryl derivatives due to an electronic overlap of the π electrons of the aryl group with the empty p_z orbitals of the boron is not reflected in the B−C bond distances in **2** compared to **1a** and **1b**. But a comparison of B−C single bonds of boron to aromatic substituents and to aliphatic ones appears to indicate that in the former they are significantly longer and support the assumption that considerable double bond character in **2** prevents chelation of the boron atoms with the adjacent carbonyl oxygens and thus the absence of thermochromicity in **2**.

The detection of a reversible solid state reaction and phase transformation described here was obviously aided by the colour changes observed. In the absence of this visual effect many similar solid state reactions have probably remained undetected. It is to be assumed that with the utilization of modern instrumentation, such as high speed DTA-DSC and X-ray methods, many analogues of this at present unique and interesting transformation will emerge.

M. Y. is grateful to the *Max-Planck-Gesellschaft* for a fellowship.

Experimental Part *)

All measurements and calculations were performed on a Syntex R 3 four circle diffractometer with a Nova 3/12 (Data General) using Nicolet P 3 and SHELXTL-software[3]. The low temperature device maintained a stability of ± 1°, the temperatures given are at the location of the sample measured before lattice determination (table 2) and data collection (ω-scan method). Structure determinations were carried out by direct methods, structure refinements by the block-cascade least squares method. Ethyl (**1a, b**) and phenyl (**2**) hydrogen atoms were calculated and refined as rigid groups with a C – H distance of 0.96 Å and unique isotropic free variable temperature parameter. Phenyl-C atoms were also refined as rigid groups with a C – C distance of 1.395 Å. No anisotropic temperature parameters were introduced to **1a** due to the poor crystal quality (thin

Table 3. Structural data for compounds **1a**, **1b**, and **2**

		1a	**1b**	**2**
Space group		$P2_1/c$	$P2_1/c$	$P2_1/c$
Molecules per unit cell		2	2	2
Density (calculated) (g/cm^3)		1.39	1.41	1.46
Number of unique observed reflexions ($F/\sigma(F) \geq R$)		364 R = 4.5	656 R = 2.5	599 R = 4.5
Scan-range (2Θ)		2.5 – 40°	2.5 – 40°	2.5 – 40°
Variable scan speed (°/min)		1.5 – 10	1.5 – 10	1.5 – 15
Peak to background ratio		1:1	1:1	1:1
Crystal dimensions (cm)		0.023 × 0.01 × 0.004	0.03 × 0.025 × 0.005	0.015 × 0.025 × 0.01
Maximum rest electron density (e/Å^3)		0.45	0.32	0.47
R-values	R	0.070	0.059	0.070
	R_w	0.072	0.065	0.075
	g	0.00345	0.00134	0.00077

$R = \Sigma(|F_o - F_c|)/\Sigma F_o$

$R_w = \Sigma((|F_o - F_c|) \cdot w^{-2})/\Sigma(F_o \cdot w^{-2})$, $w = 1/(\sigma^2(F) + g \cdot F^2)$

Table 4. Atomic coordinates and anisotropical temperature parameter as $\exp[-2\pi^2(U_{11}h^2a^{*2} + U_{22}k^2b^{*2} + U_{33}l^2c^{*2} + 2U_{12}hka^*b^* + 2U_{13}hla^*c^* + 2U_{23}klb^*c^*)]$ or $\exp[-8\pi^2U_{iso}(\sin\Theta/\lambda)^2]$ for **1a** (standard deviations in parentheses)

Atom	x	y	z	U_{11}/U_{iso}	U_{22}	U_{33}	U_{23}	U_{13}	U_{12}
C(1)	0.0504(8)	-0.2807(15)	-0.1167(7)	0.064(6)	0.032(5)	0.025(4)	0.001(4)	-0.001(4)	0.003(5)
O(2)	-0.0627(5)	-0.3636(9)	-0.1528(5)	0.066(4)	0.036(4)	0.045(4)	-0.010(3)	0.004(3)	0.000(3)
O(3)	-0.1698(9)	-0.2431(17)	-0.1089(9)	0.074(7)	0.027(5)	0.033(5)	-0.004(5)	0.005(5)	-0.007(5)
O(4)	-0.1630(5)	-0.0316(10)	-0.0166(5)	0.055(3)	0.040(4)	0.048(4)	-0.006(3)	0.006(3)	0.003(3)
C(5)	-0.0518(7)	0.0577(15)	0.0231(8)	0.063(6)	0.023(5)	0.035(5)	0.006(4)	0.013(4)	-0.002(4)
O(6)	0.1371(5)	-0.3952(10)	-0.1602(6)	0.069(4)	0.034(4)	0.052(4)	-0.005(3)	0.013(3)	0.012(3)
C(7)	-0.2934(9)	-0.3495(19)	-0.1547(11)	0.069(7)	0.075(8)	0.068(8)	-0.009(6)	-0.001(6)	-0.015(6)
C(8)	-0.3996(10)	-0.1979(27)	-0.1233(18)	0.078(9)	0.164(15)	0.259(21)	-0.123(14)	-0.060(12)	0.040(9)
H(7A)	-0.3030(9)	-0.5190(19)	-0.1155(11)	0.086(24)					
H(7B)	-0.2942(9)	-0.3580(19)	-0.2584(11)	0.086(24)					
H(8A)	-0.4767(10)	-0.2517(27)	-0.1601(18)	0.171(33)					
H(8B)	-0.4039(10)	-0.0209(27)	-0.0950(18)	0.171(33)					
H(8C)	-0.3785(10)	-0.3010(27)	-0.0410(18)	0.171(33)					

*) Further details and basic data concerning the X-ray analysis may be obtained from Fachinformationszentrum Energie Physik Mathematik, D-7514 Eggenstein-Leopoldshafen (W. Germany), by specifying registry number CSD 50461, author, and source.

plates). Additional information can be taken from Table 3, atomic coordinates and temperature factors from Table 4 – 6.

Table 5. Atomic coordinates and anisotropical temperature parameter for **1b** (details as in Table 4)

Atom	x	y	z	U_{11}/U_{iso}	U_{22}	U_{33}	U_{23}	U_{13}	U_{12}
C(1)	0.0468(3)	0.2429(7)	0.6388(4)	0.034(2)	0.018(2)	0.023(2)	-0.004(2)	0.005(2)	-0.002(2)
O(2)	-0.0450(2)	0.2351(5)	0.7093(3)	0.033(2)	0.023(2)	0.028(2)	0.003(1)	0.012(1)	0.001(1)
B(3)	-0.1518(4)	0.4198(10)	0.6888(5)	0.038(3)	0.026(3)	0.024(2)	-0.003(2)	0.011(2)	-0.001(2)
O(4)	-0.1432(2)	0.5861(5)	0.5610(3)	0.036(2)	0.032(2)	0.029(2)	0.005(1)	0.012(1)	0.002(1)
C(5)	-0.0469(3)	0.5786(7)	0.4844(4)	0.034(3)	0.024(2)	0.023(2)	-0.001(2)	0.008(2)	-0.003(2)
O(6)	0.1364(2)	0.0966(5)	0.6713(3)	0.037(2)	0.026(2)	0.024(2)	0.004(1)	0.007(1)	0.004(2)
C(7)	-0.2725(4)	0.2718(9)	0.6896(5)	0.040(3)	0.036(3)	0.042(3)	0.003(2)	0.007(2)	-0.008(2)
C(8)	-0.3813(5)	0.4430(15)	0.6764(10)	0.043(4)	0.082(5)	0.145(7)	0.029(5)	0.008(4)	0.002(4)
H(7A)	-0.2704(4)	0.1718(9)	0.7785(5)	0.056(11)					
H(7B)	-0.2814(4)	0.1582(9)	0.6059(5)	0.056(11)					
H(8A)	-0.4561(5)	0.3530(15)	0.6723(10)	0.174(24)					
H(8B)	-0.3780(5)	0.5405(15)	0.5874(10)	0.174(24)					
H(8C)	-0.3741(5)	0.5581(15)	0.7594(10)	0.174(24)					

Table 6. Atomic coordinates and anisotropical temperature parameter for **2** (details as in Table 4)

Atom	x	y	z	U_{11}/U_{iso}	U_{22}	U_{33}	U_{23}	U_{13}	U_{12}
C(1)	1.0225(4)	0.2219(13)	0.8814(7)	0.061(5)	0.051(5)	0.034(4)	0.006(3)	-0.004(3)	-0.002(4)
O(2)	0.9930(3)	0.1397(8)	0.8653(4)	0.044(3)	0.061(3)	0.053(3)	0.010(2)	0.001(2)	-0.010(3)
B(3)	0.8625(6)	0.2578(15)	0.9210(8)	0.070(6)	0.035(5)	0.038(4)	0.010(4)	-0.004(4)	-0.001(4)
O(4)	0.8778(3)	0.4684(8)	1.0044(4)	0.042(3)	0.054(3)	0.053(3)	0.001(2)	-0.005(2)	-0.012(2)
C(5)	0.9672(4)	0.5600(12)	1.0284(6)	0.056(4)	0.039(4)	0.026(3)	0.000(3)	0.001(2)	0.002(3)
O(6)	1.0796(3)	0.1100(7)	0.8299(4)	0.048(3)	0.045(3)	0.044(3)	-0.012(2)	0.011(2)	0.005(2)
C(10)	0.7648(2)	0.1496(8)	0.8926(4)	0.038(4)	0.046(4)	0.045(4)	0.007(3)	-0.005(3)	-0.007(3)
C(11)	0.7476(2)	-0.0636(8)	0.8066(4)	0.044(4)	0.058(5)	0.060(4)	0.001(4)	-0.001(3)	-0.012(4)
C(12)	0.6596(2)	-0.1597(8)	0.7795(4)	0.069(5)	0.057(5)	0.070(5)	-0.003(4)	-0.005(4)	-0.018(4)
C(13)	0.5888(2)	-0.0426(8)	0.8383(4)	0.057(5)	0.077(6)	0.081(6)	0.015(5)	-0.008(4)	-0.028(4)
C(14)	0.6060(2)	0.1706(8)	0.9243(4)	0.050(5)	0.097(7)	0.076(5)	-0.000(5)	0.008(4)	0.011(4)
C(15)	0.6940(2)	0.2667(8)	0.9515(4)	0.052(4)	0.067(5)	0.056(4)	-0.006(4)	-0.004(3)	-0.011(4)
H(11)	0.7963(2)	-0.1442(8)	0.7661(4)	0.103(11)					
H(12)	0.6477(2)	-0.3065(8)	0.7203(4)	0.103(11)					
H(13)	0.5283)2)	-0.1087(8)	0.8197(4)	0.103(11)					
H(14)	0.5573(2)	0.2512(8)	0.9649(4)	0.103(11)					
H(15)	0.7058(2)	0.4135(8)	1.0107(4)	0.103(11)					

[1] Part II: *M. Yalpani* and *R. Köster,* Chem. Ber. **116**, 3332 (1983), preceding paper.

[2] B-C bond length appears not to be a reliable criterium for the estimation of bond order. B-C single bonds range between 1.58 – 1.69 (av) Å in $(CH_3)_3B$ (*L. S. Bartell* and *B. L. Carrol,* J. Chem. Phys. **42**, 3076 (1965)) and $Mo(C_{10}H_8N_2)_2(NNMe_2)_2BPh_{42} \cdot CH_2Cl_2$ (*J. Chatt, B. A. L. Crichton, J. R. Dilworth, P. Dahlstrom, R. Gutkoska,* and *J. Zubieta,* Inorg. Chem. **21**, 2383 (1982)), and 1.58 – 1.63 Å in BBN acetylacetonate (R. Boese, unpublished results) and in $(PhBO)_3 \cdot N[CH_2CH_2]_3N$ (*M. Yalpani* and *R. Boese,* Chem. Ber. **116**, 3347 (1983), following paper).

[3] *G. M. Sheldrick,* SHEL XTL (1981). An integrated system for solving, refining and displaying crystal structures from diffraction data, University of Göttingen.

[34/83]